Journal of Volcanology and Geothermal Research 307 (2015) 107–119

Contents lists available at ScienceDirect

Journal of Volcanology and Geothermal Research

journal homepage: www.elsevier.com/locate/jvolgeores

Observations on lava, snowpack and their interactions during the 2012–13 Tolbachik eruption, Klyuchevskoy Group, Kamchatka, Russia

Benjamin R. Edwards [a,*], Alexander Belousov [b], Marina Belousova [b], Dmitry Melnikov [b]

[a] Department of Earth Sciences, Dickinson College, Carlisle, PA 17013, United States
[b] Institute of Volcanology and Seismology FEB RAS, Piip boulevard 9, Petropavlovsk-Kamchatsky 683006, Russian Federation

ARTICLE INFO

Article history:
Received 5 April 2015
Accepted 10 August 2015
Available online 29 August 2015

Keywords:
Basaltic trachyandesite
Glaciovolcanism
Lava–snow
Tolbachik 2012–13
Paleoclimate proxy
Kamchatka

ABSTRACT

Observations made during January and April 2013 show that interactions between lava flows and snowpack during the 2012–13 Tolbachik fissure eruption in Kamchatka, Russia, were controlled by different styles of emplacement and flow velocities. `A`a lava flows and sheet lava flows generally moved on top of the snowpack with few immediate signs of interaction besides localized steaming. However, lavas melted through underlying snowpack 1–4 m thick within 12 to 24 h, and melt water flowed episodically from the beneath flows. Pahoehoe lava lobes had lower velocities and locally moved beneath/within the snowpack; even there the snow melting was limited. Snowpack responses were physical, including compressional buckling and doming, and thermal, including partial and complete melting. Maximum lava temperatures were up to 1355 K (1082 °C; type K thermal probes), and maximum measured meltwater temperatures were 335 K (62.7 °C). Theoretical estimates for rates of rapid (e.g., radiative) and slower (conductive) snowmelt are consistent with field observations showing that lava advance was fast enough for `a`a and sheet flows to move on top of the snowpack. At least two styles of physical interactions between lava flows and snowpack observed at Tolbachik have not been previously reported: migration of lava flows beneath the snowpack, and localized phreatomagmatic explosions caused by snowpack failure beneath lava. The distinctive morphologies of sub-snowpack lava flows have a high preservation potential and can be used to document snowpack emplacement during eruptions.

© 2015 Elsevier B.V. All rights reserved.

1. Introduction

Interactions between volcanism and the cryosphere, broadly called 'glaciovolcanism', are increasingly recognized as a critical topic for understanding planetary processes (e.g., Edwards et al., 2009; Tuffen and Betts, 2010; Wilson et al., 2014; Edwards et al., 2015). Over 180 active volcanoes on Earth have at least some permanent ice cover (Edwards et al., 2014); as demonstrated during the 2010 eruption at Eyjafjallajökull in southern Iceland, eruptions at ice-clad volcanoes can produce unique hazards like phreatomagmatic explosions and various water-based hazards such as jökulhlaups (Major and Newhall, 1989; Roberts, 2005; Gudmundsson et al., 2008, 2012; Belousov et al., 2011; Waythomas et al., 2013). Our increasingly complex attempts to model the distribution of Pleistocene ice cover during glacial stades require improved accuracy in determining the distribution of ice on Earth, the timing of ice cover, and the thickness of ice cover. In parts of Antarctica, Iceland, and British Columbia the most accurate records for pre-Last Glacial Maximum glaciations are derived from glaciovolcanic deposits (e.g., McGarvie et al., 2006; Smellie et al., 2008; Edwards et al., 2011). These same paleoclimate tools have increasingly been applied where possible to assist with reconstruction of planetary climate history for Mars (e.g., Allen, 1979; Head and Wilson, 2007; Scanlon et al., 2014, 2015) and for identifying targets for biological exploration of Mars (e.g., Cousins et al., 2013).

Most research on glaciovolcanism has focused on ancient deposits, but two new research avenues are emerging. One is large-scale experiments that investigate heat transfer from lava to ice (Schmid et al., 2010; Edwards et al., 2013b) and the textures and morphologies of scaled lava–ice interactions (Edwards et al., 2013b). These experiments better quantify the heat balance controlling rates of ice melting, document the ease of gas penetration into lava, and also the complex role of steam in buffering the boundary zone temperatures when a substrate separates lava from ice. A second avenue for new research is a series of well-documented eruptions in Iceland (e.g., 1996 Gjálp: Gudmundsson et al., 1997, 2004; 1998/2004 Grimsvötn: Jude-Eton et al., 2012; 2010 Eyjafjallajökull/Fimmvorduháls: Magnusson et al., 2012; Gudmundsson et al., 2012; Edwards et al., 2012). Some qualitative observations of lava–snow interaction were made during earlier eruptions, especially the 1947 Hekla eruption (Einarsson, 1949; Kjartansson, 1951). But the recent observations have quantified both long and short-term heat transfer (e.g., Gudmundsson et al., 2004), characteristics of tephra

* Corresponding author. Tel. +1 717 254 8934.
E-mail address: edwardsb@dickinson.edu (B.R. Edwards).

http://dx.doi.org/10.1016/j.jvolgeores.2015.08.010
0377-0273/© 2015 Elsevier B.V. All rights reserved.

deposits (e.g., Jude-Eton et al., 2012), and difference in types of lava–snow/ice heat transfer (e.g., Edwards et al., 2012).

An eruption on the southern rift zone of the Tolbachik volcanic massif (Edwards et al., 2014; Belousov et al., 2015; Fig. 1) from November 2012 to September 2013 allowed observations of interactions between various lava flows and snowpack. Initial snow cover at the main eruptive fissures (Menyailov vents at 1900 m a.s.l. and Naboko vents at 1650 m a.s.l.) was less than 1 m, but during the following five months it deepened to greater than 4 m locally. Ground and aerial images from the first six months of the eruption show voluminous steam produced as lava flowed over snow. Here we detail field observations from several months at Tolbachik, including measurements of lava temperatures, meltwater temperatures, variations in lava behavior, variations in snowpack response, and characterization of deposits formed by direct and indirect lava–snowpack interactions. We also compare the observations from Tolbachik with those from other recent eruptions, experiments, and modeling of heat transfer between lava and snow/ice.

2. Methods

Most data presented here are based on relatively simple field observations and measurements. Relatively low effusion rates after December 2012 made possible close field observations of lava morphologies and processes at developing contacts between lava and snow. Snowpack depths in front of advancing lava flows were estimated with a snow probe, and photography and videography documented rapid changes to snow and lava flows. We estimated snow density by melting measured volumes of snow in a graduated container.

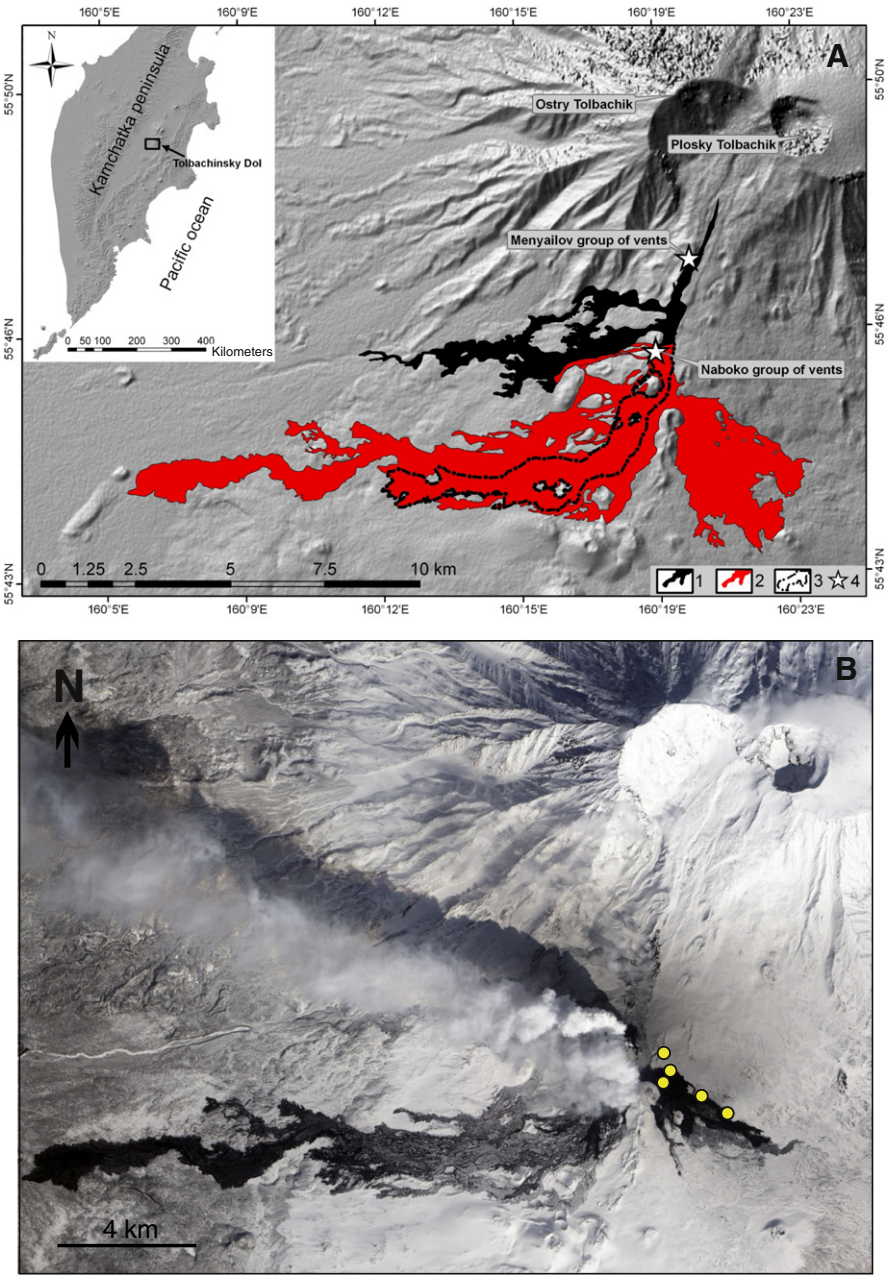

Fig. 1. Location maps of the 2012–13 Tolbachik fissure eruption; inset shows the location of the Klyuchevskoy Group on the Kamchatka Peninsula. A. Map showing final distribution of lava flows and both vent clusters. B. Satellite image from February 2012 highlighting the extent of snowcover at the eruption site with locations of detailed lava–snowpack observations shown as yellow dots.

We measured temperatures of lava flows and meltwater periodically with type K thermal probes connected to an OMEGA data logger. Probes were inserted into lava flow surfaces at depths up to ~20 cm and temperatures were recorded at 2 s intervals; typically maximum temperatures were recorded within 60 s. We also measured surface temperatures of lava flows, meltwater streams, and ground surface using Forward Looking Infrared (FLIR) cameras. Air temperature and humidity measurements facilitated FLIR temperature corrections.

We dug snow pits in four places to measure and sample ash stratigraphy and to observe snowpack response to being overridden and intruded by lava flows. The pits allowed three-dimensional views of lava–snowpack interactions and meltwater production and movement within the snowpack. Measurements of snowpack thicknesses between ash layers also allowed us to qualitatively document snowpack growth during the eruption.

3. Results

3.1. Observations of lava–snowpack interactions

Three styles of lava–snowpack interaction were observed during the eruption (Edwards et al., 2014; Fig. 2), involving: i) `a`a flows (Figs. 2 and 3), ii) sheet flows (Figs. 2 and 4), and iii) pahoehoe flows (Figs. 2 and 5). In the first, lavas move with a caterpillar-track motion, where a lens of lava breccia (`a`a; Fig. 2A) or an outer chilled skin of lava (sheet flows; Fig. 2B) rolls over the top of the snow. The combination of this track-like motion style and moderate flow velocities (>0.025 m s^{-1}) allowed these two lava types to readily move on top of snow, even when migrating upslope (Fig. 3D).

Most of the detailed observations were made along the edges of the eastern lava field in February–April 2013 that flowed from the Naboko vents. February's first major lava advance to the east began, but stopped; another began in March and lasted until mid-April (Fig. 1). Each of these lava advances occurred through snowpack 1–4 m deep.

`A`a flows: The dominant lava flow morphology in January through April 2013 was `a`a, especially at medial and distal ranges (Belousov et al., 2015). During the initial stages of the eruption high discharge rates (>400 m^3 s^{-1}) generated fast flows that advanced up to 9 km in 24 h (~0.1 m s^{-1}). But, during most of our observations in March–April 2013, flow velocities were only <0.03 m s^{-1} (<0.1 km h^{-1}). The thickness of flows emplaced on top of the snowpack varied from 1 to 6.5 m (Fig. 3A, B). On steeper slopes (>3°) the flows formed more elongate lobes and channels bounded by lava–rubble levees or bounded by snowpack as flows slowly melted through the snow. On gentler slopes (<3°) flows spread longitudinally but also laterally. Locally they migrated upslope on the snowpack (Fig. 3C). The leading snout of the flows

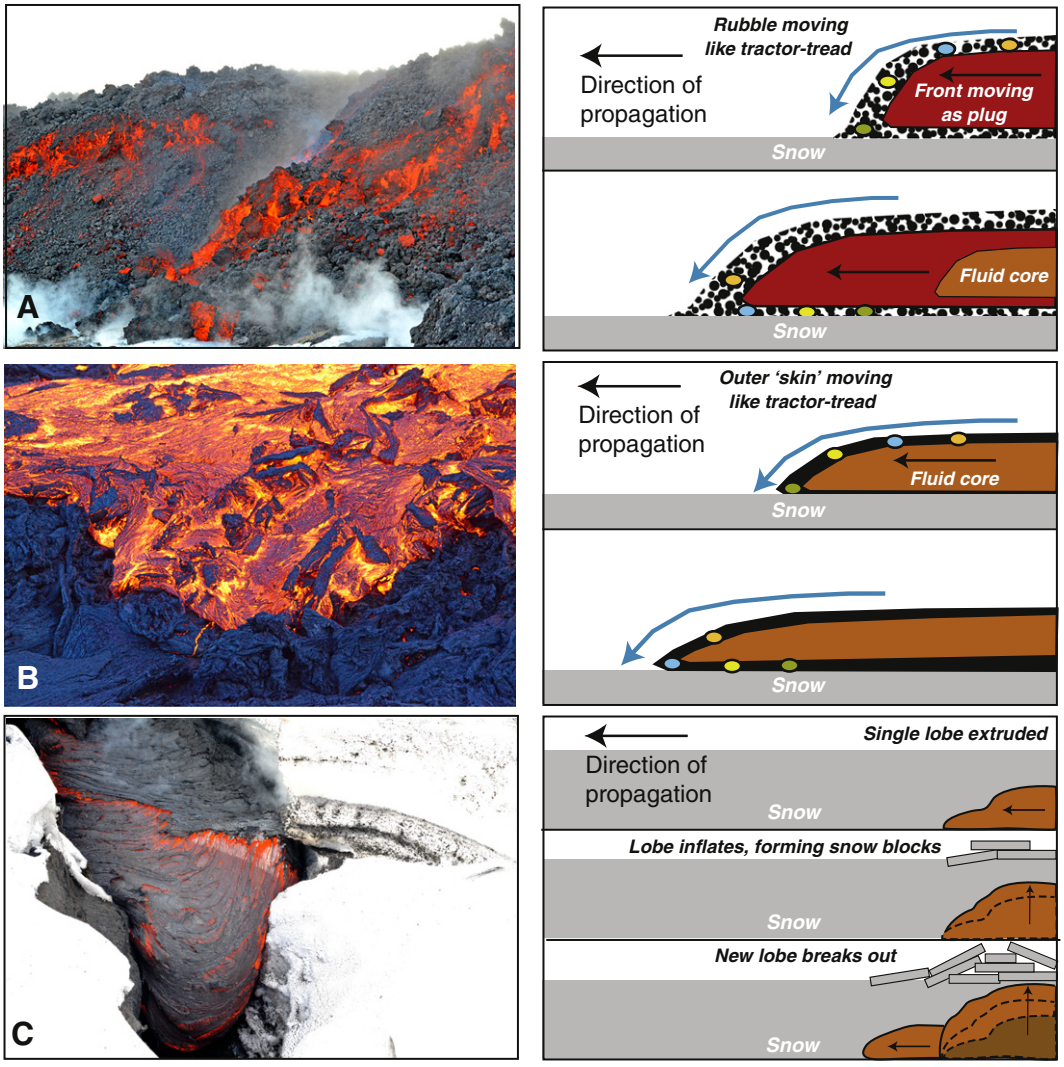

Fig. 2. Three main types of lava flow emplacement observed during lava–snow interactions. A. Advance of `a`a lava flow on top of snow; upper autobreccia carapace moves in a tread-like motion. B. Advance of sheet flow on top of snow; coherent outer lava 'skin' moves in a tread-like motion. C. Advance of pahoehoe/toothpaste flow by extrusion, inflation and subsequent breakout.

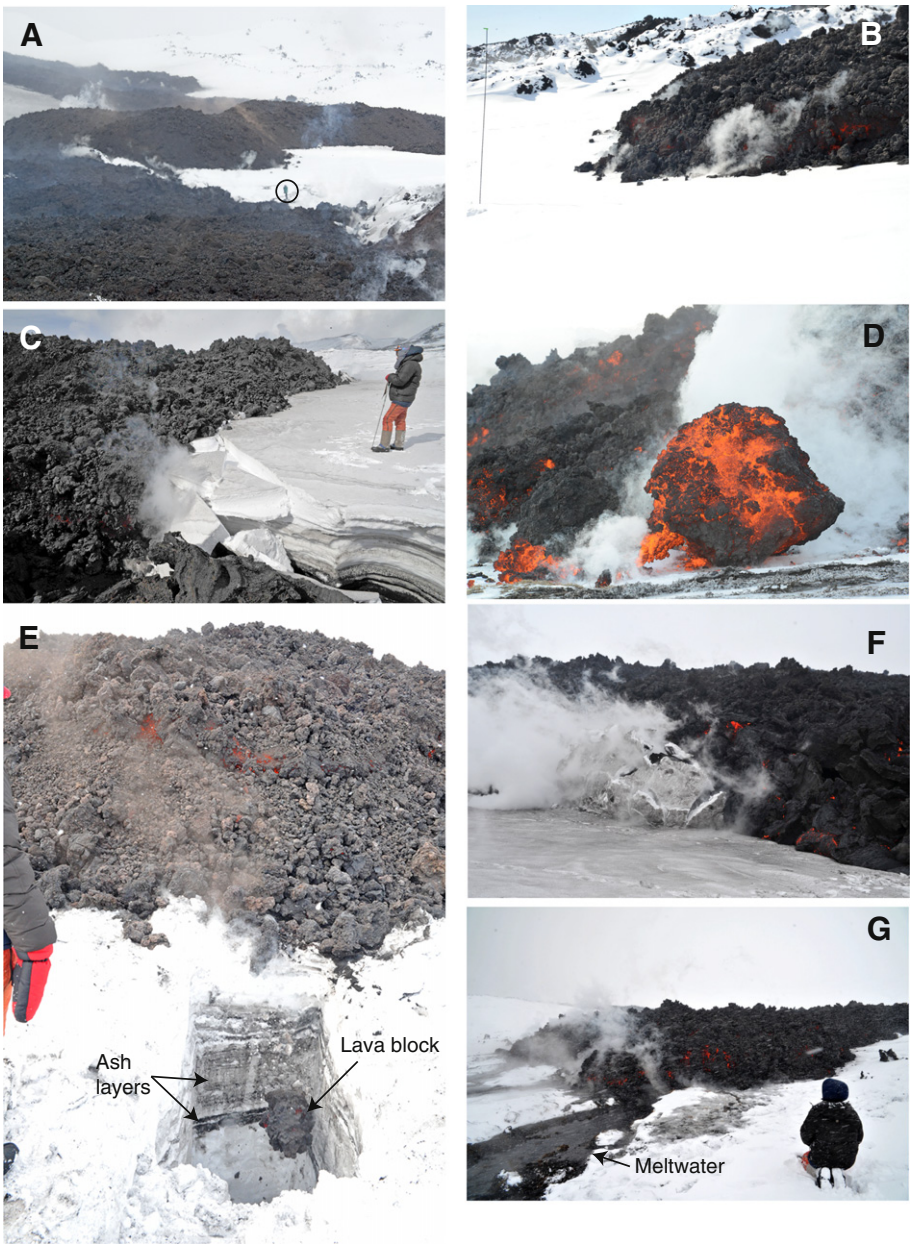

Fig. 3. Field images of `a`a lava–snowpack interactions. A. Large (>20 m wide), thick (>5 m) `a`a lava lobes moving across the top of snow ~3 m thick. Person in circle for scale. B. Small (~5 m wide) `a`a lava flowing down slope (~6°); steaming from incandescent block rolling onto snow. Two-meter snow probe for scale. C. Front of advancing `a`a lava moving into snowpit, which is ~1 m across and 2.5 m deep. Partly radiant block from lava front in the bottom of the pit; ash stratigraphy visible in pit walls. D. `A`a lava moving upslope across snow. Person for scale. E. Large (~1 m) incandescent block from advancing `a`a front producing steaming. F. Slowly advancing (<1 m min^{-1}) `a`a flow bulldozing snowblocks from lava–snow contact. Lava front ~2 m high. G. Meltwater stream exiting from the front of an advancing `a`a lava. Person for scale.

typically showed the most incandescence, while tabular, mostly solidified plugs of lava rode in the middle of the flow advancing on top of a thick rubble lens and covered by rubble. It was difficult to directly measure the thickness of the basal breccia, but it is estimated to have generally been up to one-third of the total flow thickness or less (<2 m).

The `a`a flows and the snowpack interacted thermally and physically. Steam and meltwater formed by thermal interactions appeared at different times and locations. Steam was mainly at the leading edges and sides of advancing flows, where rapid heat transfer from incandescent blocks made steam 'puffs' (Fig. 3D). In snowpack observation pits dug in front of advancing `a`a flows (Fig. 3C) little direct melting was seen. But, in one pit we did see transient within-snowpack water flows, and in several locations episodic meltwater floods were observed (Fig. 3E). We measured water temperatures up to 50 °C. Lava channels developed within deep snow (>4 m), where the tops of the flows were below the top of the snowpack, showing that over time channels melted through snow. Advancing `a`a flows at times broke snowpack into blocks and pushed them along in front of advancing lava (Fig. 3F).

Sheet flows: Sheet flows are lobes of relatively fast moving lava whose outer surface is a nearly continuous skin (unlike the broken surface of `a`a) that also has a caterpillar-track style of motion. However, they lack a rubbly flow bottom breccia. They were only observed in one proximal part of the Tolud lava field (Fig. 1B), which was continuously fed by a bocca (Fig. 4A, B). Sheet flows developed periodically when the lava channel became blocked by one or more accretionary lava balls. Lava within the channel then rose until it overtopped channel levees and flowed as a sheet across older flows, many of them covered by 10 to 20 cm of snow (Fig. 4C). Sheet flows large enough in volume left the northern side of the lava field across undisturbed snowpack

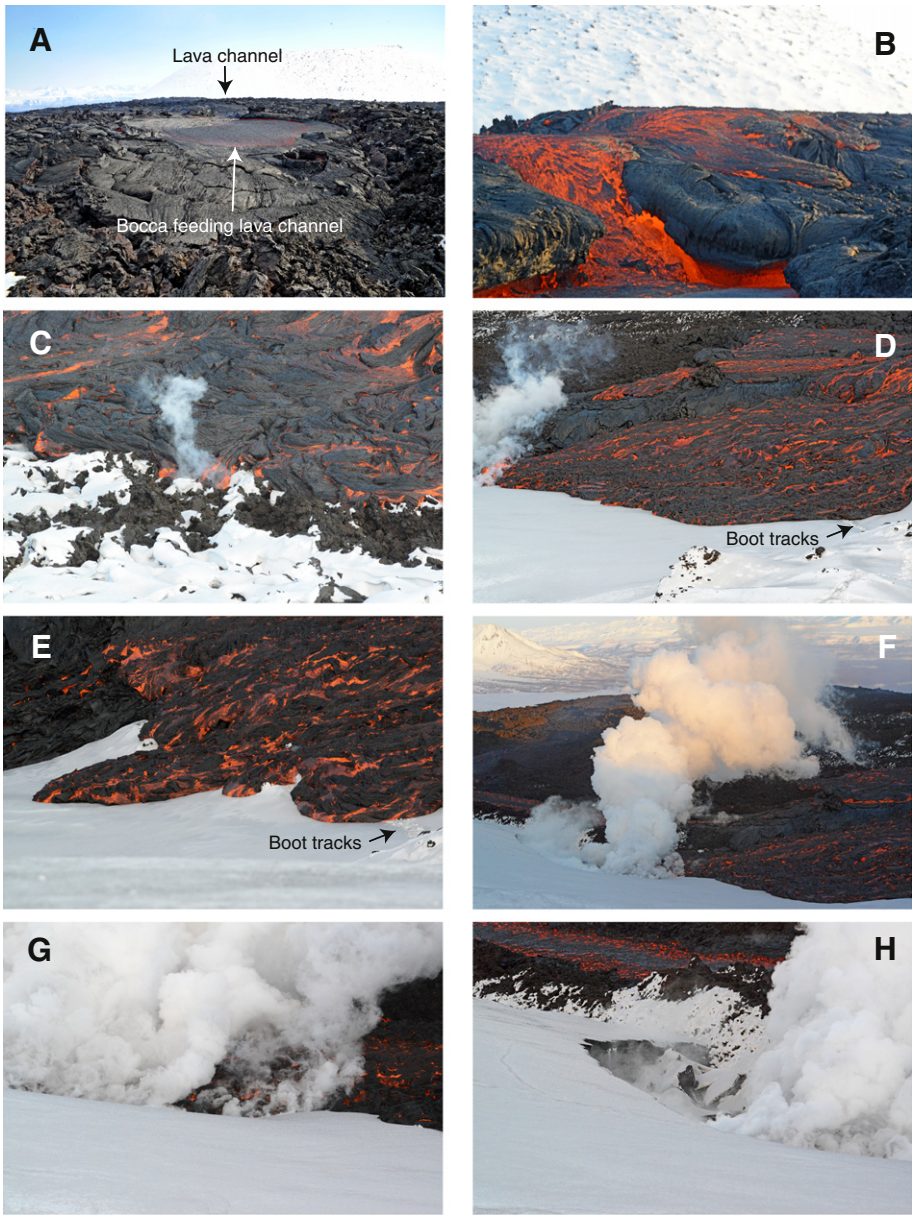

Fig. 4. Field images of sheet lava–snowpack interactions. A. View of bocca, ~25 m wide, in proximal eastern lava field that fed sheet flows. B. View of lava channel beginning to overflow. Channel is ~5 m wide. C. Broad lava sheet advancing across snow-covered, older slabby pahoehoe flow. Field of view is approximately 30 m across. D. Broad lava sheet advancing across subhorizontal, thick (<4 m) snowpack. Field of view approximately 50 m. E. Lobes at front of sheet lava flowing down slope onto thick snowpack. Foot trail through snow for scale. F. Distant view of steaming where sheet lava contacts snow. Field of view is approximately 100 m. G. Closer view of intense steaming from meltwater draining on to the surface of sheet flows. Field of view is approximately 30 m. H. Close-up of pit melted in deep (>4 m) snow with visible blocks that have broken off and are melting on top of lava. Embankment is approximately 4 m high.

(Fig. 4D). Atop the snow sheet, flows 1–2 m thick moved up to ~0.4 km h^{-1}. On slopes the sheets locally separated into separate lobes (Fig. 4E), but then merged together where slopes decreased (Fig. 4F).

Generally sheet flows and snow did not immediately interact. Flows moving across thin, isolated patches of snow made steam (Fig. 4C) but across thick snowpack almost no interaction occurred (Fig. 4D). Interactions were more vigorous where a sheet flow encountered vertical walls of snow. In one area referred to informally as the 'steam pit' the snow was exceptionally thick (>4 m) and lava accessed the edge of the snowpack (Fig. 4F, G). Because the lava flows were ~1 m thick, as they melted into the snowpack they oversteepened the snow so that it foundered onto the advancing lava flow, and made abundant steam (Fig. 4H).

Pahoehoe flows: True pahoehoe lava (Fig. 5A), whose surface remains elastic and stretches during inflation, was intimately intermixed with lava lobes whose surface fractured during inflation (Fig. 5B–D). The second type generally has partial lineations on their surfaces and locally 'spiny' surfaces (Fig. 5D), which are characteristic of 'toothpaste' lava (Rowland and Walker, 1987). But, estimated viscosities calculated for eruption temperatures and crystallinities/bubble densities well beyond those estimated for Tolbachik flows (<0.3; Volynets et al., 2015) vary from 10^3 to 10^4 Pa s, which is below the threshold for the pahoehoe–toothpaste transition as defined by Rowland and Walker (1987; $>10^4$ Pa s). It may be that this rigid-skin variant of pahoehoe represents a transition between elastic-skin pahoehoe and toothpaste lava. For both types inflation dominates lava lobe growth. They moved at the slowest observed velocities (<0.001 m s^{-1}/<4 m h^{-1}). These lava types were found mainly in proximal to medial areas of low slope, and formed after the initial passage of the main lava flow fronts. Some flowed into moats formed between the `a`a flow edge and the snowpack by snow melting. Like the sheet flows they do not produce a basal lava

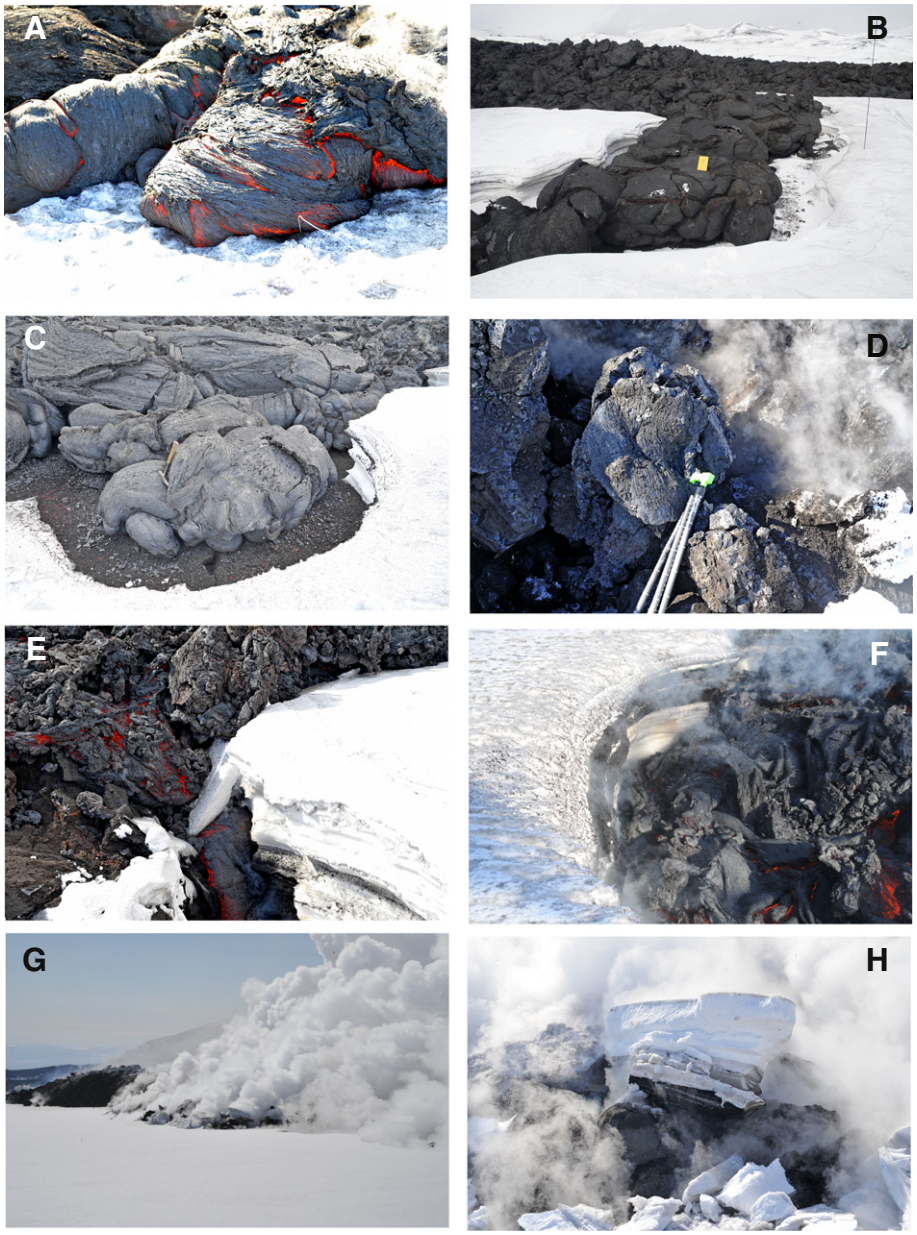

Fig. 5. Field images of pahoehoe–snow interactions. A. Pahoehoe toe inflating on top of snow. Lobe is ~1 m long. B. Mass of individual pahoehoe toes forming a small lava lobe. Notebook for scale is 15 cm. C. Closer view of pahoehoe lobes separated by moat from relatively thin (<1 m thick) snow. D. Pahoehoe lobe inflating up through snowpack; lineations are visible on lava surface. Folded snowprobe is 50 cm long. E. Small (~30 cm wide) pahoehoe toe moving into moat in snow and melting small block of snow. F. View looking down into moat being filled by inflating pahoehoe toes. Field of view is ~3 m. G. Steam rising from on top of pahoehoe lava toes migrating through moderately thick (~2 m) snow. `A`a lava to the left of steam is ~3 m high. H. Lava toes pushing blocks of snow up. Field of view is ~4 m.

breccia but directly contact their substrate. Individual lobes are generally l to 2 m long and advance by sequential breakouts (Fig. 5B, C).

Although pahoehoe lavas were volumetrically minor compared with `a`a, their mode of emplacement made possible close observations of their interactions with snow. These lavas were seen abutting the vertical edge of the snowpack (Fig. 5E), interacting with individual snowblocks (Fig. 5F), and migrating beneath the surface of the snow making steam curtains (Fig. 5G) and uplifting snowblocks (Fig. 5H). Contact between lava flow surfaces and snowpack did produce visible melting at the interface, but melting was so slow that individual snowblocks slowly melted (>60 s) and were compressed (Fig. 5F). We dug an observation pit dug directly in front of an advancing compound pahoehoe flow that was ~2.3 m deep, 2 m wide, and 3 m long (Fig. 6A) to better see the lava–snow interactions. As the base of the lobe came within ~1 m of the proximal pit wall, the snowpack began to fracture subvertically and protrude into the pit (Fig. 6B, C). The snow became saturated with meltwater, with little to no steaming (Fig. 6B). But, after the advancing lobe penetrated the base of the pit, meltwater from the overlying snow dripped onto the inflating lobe making much steam (Fig. 6D). After ~2 min the flow fractured/melted the proximal pit wall, and small pahoehoe breakouts inflated and filled the observation pit (Fig. 6E, F). The upper part of the proximal wall detached block and was partly uplifted by the inflating lobes.

3.2. Snowpack behavior

Physical interactions produced compressional and extensional features. Compression caused shortening including piles of upturned snowblocks at the interface of `a`a and the snowpack (Fig. 7A, D) and folding/buckling of surface layers up to several meters away from the

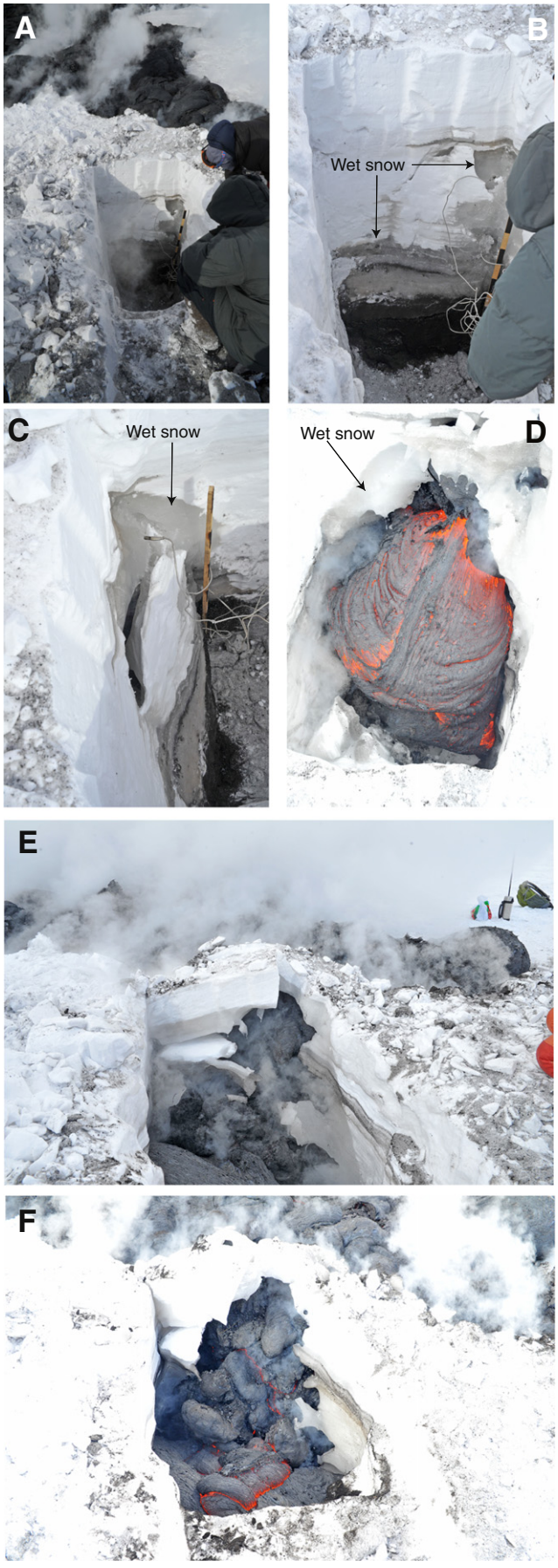

interface (Fig. 7B, C). Vertical extension formed snow domes (Fig. 7E, F), and fractures parallel to vertical snowbank faces became detachment surfaces for snowblocks that fell onto lava flanks from oversteepened vertical faces (Fig. 7G). Crushing and compaction of snow was audible as flows advanced over it.

Thermal interactions made copious steam (Fig. 7H) and occasionally meltwater (Fig. 7I–L). Steam plumes accompanied snow domes where lava migrated beneath the snow (Fig. 7F, H); they were also common in front of rapid `a`a flows. Meltwater formed beneath supra-snow lava flows (e.g., Fig. 6B) and exited at flow fronts (Fig. 7J–L), but also as ephemeral lenses in snow (Fig. 7I). In one 3.62 m deep snow pit the lowest 1.65 m was initially water saturated, but the water level decreased by 0.20 m in 30 min. Meltwater drained in pre-existing gullies (Fig. 7J), or smaller, more temporary 'floods' from the fronts of advancing lava flows (Fig. 7K–M). The water was up to 62 °C (Table 2), and it melted channels through snow (Fig. 7N). Draining meltwater passed from uphill to downhill lava flows to make steam curtains (Fig. 7L).

3.3. Lava temperatures

The temperatures of lava cores from toothpaste lobes were measured to be as high as 1355 K (1082 °C), and the average of the 10 highest independent temperature measurements was 1332 K (1059 °C; standard deviation 20.6°; Tables 1 and 2). Temperatures within radiant blocks from the fronts of `a`a flows were lower (up to 1276 K/1003 °C). For comparison, the estimated liquidus temperature calculated using rhyolite-MELTS (Gualda et al., 2012) for a series of samples of fresh lava that span the entire eruption period (see Volynets et al., 2015) is 1419 K (1146 °C; estimated average density of 2615 kg m^{-3}). Temperature estimates from FLIR were up to 1342 K (1069 °C) for radiant cracks in lava surfaces.

3.4. Snowpack and meltwater characteristics

Snowpack and meltwater measurements include estimates of snow density, meltwater temperatures (Table 2), and depths of snow. Snow densities from three samples had values of 388, 459 and 526 kg m^{-3}, with implied porosities of 58%, 50% and 43%. Estimates of snow temperatures from FLIR images ranged from 273 to 264 K (0 to −9 °C). Melt water temperatures in two locations were up to 335.7 K (62.7 °C; Table 2).

Four snowpits documented snow depths and stratigraphy of ash layers. We dug the first pit (6180300 N/583350E; 26 January 2013) ~1 km from the Naboko vents through 2.5 m of snow. At this location it had 4 layers of lapilli, and three zones of disseminated ash and lapilli. The base of the snow had no ash or lapilli. The second snow pit (6178918 N/584820E; 3 April) was ~3.5 km east of the Naboko vents on a flat bench and was 3.65 m deep. The lowest 1.65 m was water saturated and did not have ash or lapilli, but had 3 layers of ash above. The third pit (6178749 N/585436E; 6 April) was 4 km east of the Naboko vents on sloping snow and was 2.4 m deep. The lowest 1 m lacked ash but had 3 layers above. The last pit (6179850 N/583600E; 9 April) was ~1.5 km east of the Naboko vents and 2 m deep. The lowermost 1.2 m had no ash or lapilli, but was overlain by three layers of coarse ash/lapilli.

Fig. 6. Field images showing sequence of pahoehoe lava breaking into snowpit. The pit is ~1 m wide. A. View showing the top of pahoehoe lobe protruding above the snow surface and beginning to break through wall of pit. Black bars on scale stick are 10 cm long. B. View showing pit wall proximal to lava flow; flow has entered the base of the pit, and meltwater, indicated by wet snow, is migrating through the snowpack ahead of the lava. C. View looking down on the pit wall closest to the lava showing slab of snow that has fractured and is being pushed into the pit. D. Pahoehoe toe inflating into the pit. E. View of pit proximal to the advancing flow; pit wall is failing and inflating lava is uplifting blocks of snow. F. View looking at the bottom of the pit with numerous lava toes beginning to infill the open pit.

4. Discussion

Interactions between lava flows and snow/ice have been observed and recorded in the field since the 1947 Hekla eruption (Einarsson, 1949; Kjartansson, 1951). From those first observations the interactions have been unexpected and enigmatic. Early workers were shocked at the seeming inability of lava flows to have immediate impacts on snow, as they watched flows migrate on top of snowpack as though the snow were a non-meltable substrate. But, this seemingly surprising behavior has been predicted by thermal modeling (e.g., Wilson and Head, 2007), repeated during large-scale experiments (Edwards et al., 2013b), and repeatedly seen in the field during other eruptions (1994 Klyuchevskoy: Belousov et al., 2011; 2010 Fimmvorduháls: Edwards et al., 2012; many eruptions at Mt. Etna: B. Behnke, pers. comm, 2014; U. Kueppers, pers. comm., 2012).

4.1. What controls whether lava moves on top or beneath/through snowpack?

The main observations on lava flows migrating across or within snowpack/ice are these. (1) Lavas whose advance is dominated by caterpillar-track motions travel on top of the snowpack (Edwards et al., 2014). (2) Lavas that advance at rates more than 30 m h^{-1} also travel on top of the snowpack (Edwards et al., 2012). (3) Lavas with basal flow breccias flow on top of snowpack (Einarsson, 1949; Kjartansson, 1951; Edwards et al., 2012). (4) Lavas with access to ice/

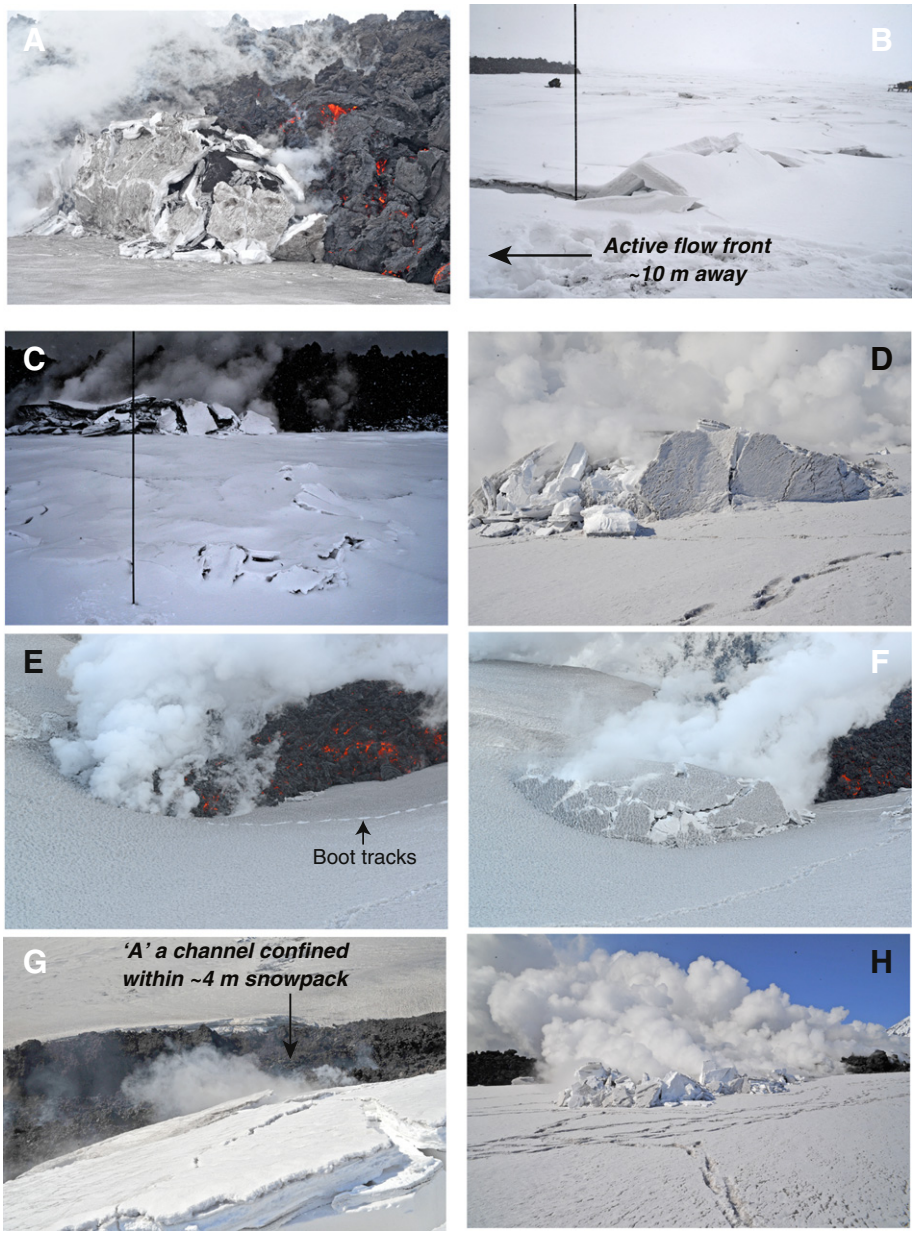

Fig. 7. Field images of snow responses to interactions with lava. A. `A`a lava uplifting thin plates of snow. Lava is ~2.5 m high. B. Thin plates of snow buckling into antiform. Snowprobe for scale. C. Ridges formed in snow by lava flow advance. Snowprobe for scale. D. Thick blocks of snow broken by advancing lava. E. Steaming pit in thick (>4 m) snowpack being invaded by sheet lava. Boot tracks in snow for scale. F. Large (>10 m in diameter) dome in snow formed by within-snowpack lava inflation. Boot tracks for scale. G. Large (>3 m thick) snowblock fracturing from thick (>4 m snowpack) along edge of `a`a flow channel. H. Field of snow slabs being pushed up by lava flows. Note large steam plumes forming as snow melts and drains down into underlying lava. I. Meltwater migration immediately beneath the snow surface visible in disrupted snow. `A`a flow in the background is ~5 m thick. Boot tracks in mid-ground for scale. J. Narrow channel eroded into snow by small flood. Channel is ~50 cm deep. Meltwater streaming from beneath advancing `a`a lava. Person for scale. K. Meltwater channel forming in thin snow (~50 cm thick) during drainage event from beneath `a`a lava. Channel is ~2 m wide. L. Meltwater streaming from beneath upslope `a`a lava down into older flow. Stream is ~5 m wide.

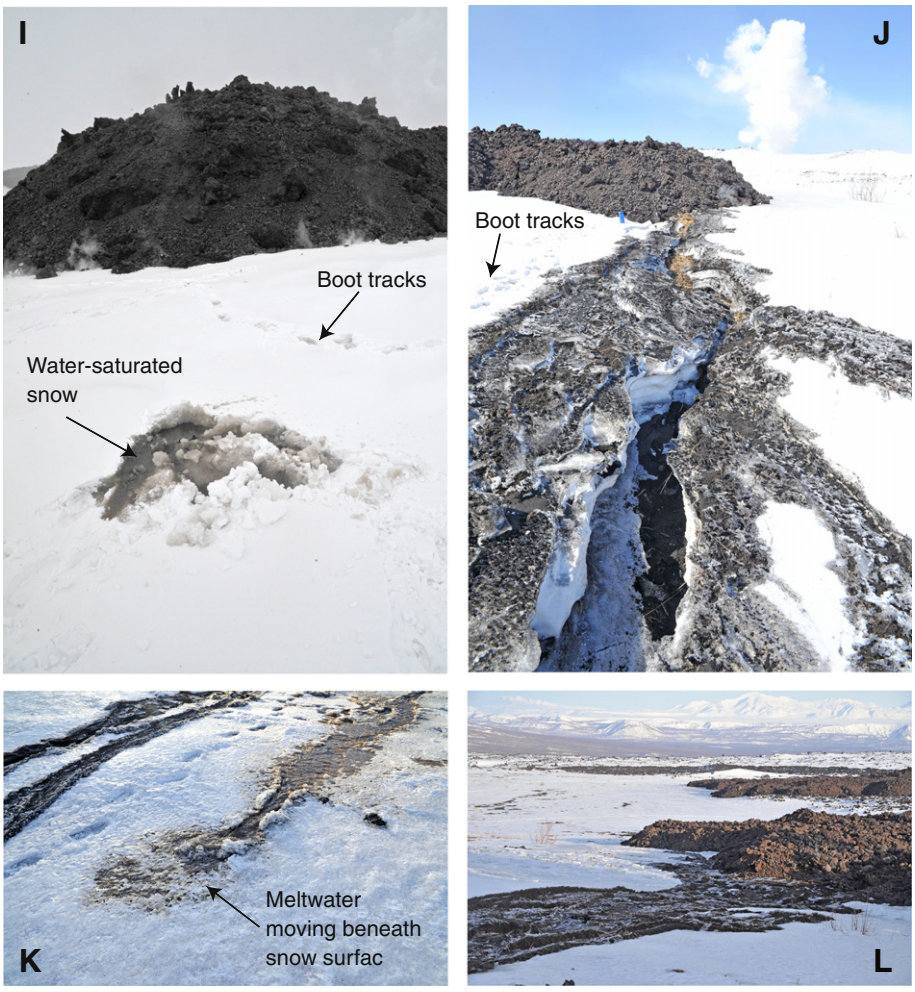

Fig. 7 (*continued*).

snowpack-substrate contact travel there (1991 Llaima: Moreno and Fuentealba, 1994; 1991 Hudson: Naranjo et al., 1993; 1971 Villarica: Naranjo and Moreno, 2004; 1984 Hekla: Gronvold et al., 1983; 2010 Gigjökull: Oddsson et al., 2012; Edwards et al., 2014). (5) Slow moving (<30 m h^{-1}) lava flows where inflation rates are of the same magnitude as advance rates can move beneath/through the snowpack. (6) While most snow is eventually melted by supra-snowpack lava flows, melting is generally much slower (maximum ~5 m day^{-1}) than lava advance rates (Einarsson, 1949; Kjartansson, 1951; Edwards et al., 2012, 2013a,b). Essentially all of these observations are explained by either thermal or physical mechanisms. The time-scales of heat transfer rates between lava and snowpack/ice have been explored by several workers

Table 1
Summary of lava temperature measurements made in the field.

Experiment number	Date	Maximum reading (K)	Maximum reading (°C)	Notes
1-01	22-Jan-13	1004	731	Temperature on the surface of isolated lobe
1-02	22-Jan-13	1309	1036	Internal temperature of isolated lobe inserted ~5 cm beneath surface
2-01	1-Apr-13	1349	1076	Temperatures measured in lava advancing through snow
	1-Apr-13	1329	1056	Temperatures measured in lava advancing through snow
2-02	1-Apr-13	1355	1082	Temperatures measured in lava advancing through snow
	1-Apr-13	1354	1081	Temperatures measured in lava advancing through snow
2-03	1-Apr-13	1331	1058	Temperatures measured in top of lava; first probe inserted
	1-Apr-13	1212.4	939.4	~4 cm into flow top, second inserted ~2 cm into flow top
2-04	1-Apr-13	1319	1046	Temperature measured in lobe extruded into observation pit (Fig. 6D)
2-05	1-Apr-13	1276	1003	Temperature measured in radiant crack in `a`a flow (ST02)
		797.9	524.9	Temperature measured at left-side base of `a`a flow (ST02)
		644	371	Temperature measured at middle base of `a`a flow (ST02)
2-06	1-Apr-13	1353	1080	Temperature measured in small lobe at base of larger `a`a flow
2-08	2-Apr-13	1207	934	Temperature measured at side of small lava channel
2-09	2-Apr-13	1295	1022	Temperature measured at side of small lava channel
2-11	2-Apr-13	1328	1055	Temperature of lava flow ~10 m north of meltwater stream (see Exp 2-10, Table 2)
2-12	3-Apr-13	938.6	665.6	Temperatures measured in cracks of blocks on front of advancing `a`a flow
	3-Apr-13	1150.1	877.1	Temperatures measured in cracks of blocks on front of advancing `a`a flow
	3-Apr-13	1171.9	898.9	Temperatures measured in cracks of blocks on front of advancing `a`a flow

Table 2
Summary of water temperature measurements made in the field.

Experiment number	Date	Maximum reading (K)	Maximum reading (°C)	Notes
2-04	1-Apr-13	311.7	38.7	Temperature measured in water-saturated snow in observation pit
2-10	2-Apr-13	330.8	57.8	Temperature measured in meltwater stream (ST06)
	2-Apr-13	324	51	Temperature measured in meltwater stream (ST06)
	2-Apr-13	335.7	62.7	Temperature measured in meltwater stream (ST06)
	2-Apr-13	334.2	61.2	Temperature measured in meltwater stream (ST06)
	2-Apr-13	311.7	38.7	Temperature measured in meltwater stream (ST06)

(e.g., Höskuldsson and Sparks, 1997; Wilson and Head, 2007; Edwards et al., 2012). The fastest method of transferring thermal energy is via radiation, and Edwards et al. (2012) showed that melting due to radiative heat transfer results in maximum melting rates of ~5 m h^{-1} for basaltic lavas (T_{lava} = 1473 K/1200 °C). For Tolbachik lavas (T_{lava} = 1373 K/1100 °C) we estimate that the maximum radiant melting rate would be ~2 m h^{-1} (Fig. 8). Observed downslope lava velocities at Tolbachik were on the order of ~10 m h^{-1} (Fig. 8), which means that 'sinking' of lava into the snowpack/ice only occurred slowly, and was unlikely to be noticeable at the accessible/visible fronts of lava flows where radiant heat transfer is most likely to be dominant. Alternatively, conductive heat transfer will be the slowest form of heat transfer (Edwards et al., 2012), and for thin lava flows with thin basal breccias heat fluxes produce melting rates that are less than ~0.5 m h^{-1} (Fig. 8; Wilson and Head, 2007). Because air has a much lower thermal conductivity (0.025 W m^{-1} K^{-1} at 273 K; reported in DeWalle and Rango, 2008) than rock (~2 W m^{-1} K^{-1} at 273 K) or ice (2.23 W m^{-1} K^{-1} at 273 K; reported in DeWalle and Rango, 2008), air present in either basal lava breccia or in snow inhibits heat transfer. Field observations show that lava flows can rapidly melt through ice (e.g., 1991 Hudson; Naranjo et al., 1993), presumably because ice has less trapped air than snow. But, most observed rates of lava emplacement during glaciovolcanic eruptions are higher than rates of melting for any style of heat transfer, indicating that many lavas simply move too fast to melt ice out of their paths (Fig. 8). The exception to this at the Tolbachik eruption was the 'rigid-skin' pahoehoe lava, whose rates of advance were very similar (but slightly higher) than radiant heat transfer rates; they remained within the snowpack.

In instances where lava flows have been observed to move beneath ice (1991 Llaima: Moreno and Fuentalba, 1994; 1991 Hudson: Naranjo et al., 1993; 1971 Villarica: Naranjo and Moreno, 2004; 1984 Hekla: Gronvold et al., 1983; 2010 Gigjokull: Oddsson et al., 2010; Edwards et al., 2014), or ancient lava flows have been inferred to have moved beneath ice (Hungerford et al., 2014), the movements may have been facilitated by openings at the base of the ice. Röthlisberger-channels (R-channels; extending up into the overlying ice) and Nye-channels (N-channels; extending down into sub-ice substrate) are two commonly recognized types of cavities where sub-ice drainage occurs (Cuffey and Paterson, 2010). Access to pre-existing structures would allow faster sub-ice movement while minimizing the need for melting.

4.2. What controls the production of steam during lava–snowpack interactions?

Given the high heat capacity (C_p; ~1200 J kg^{-1} K^{-1} for silicate melts and glasses over a range of temperatures; Spera, 2000) and the large temperature interval over which lava cools to ambient temperatures (~1200 K), the sensible heat alone available from the cooling of 1 kg of lava from eruption to ambient temperatures releases enough heat (~1.4×10^6 J) to melt between 3 and 5 times its mass of ice (latent heat of fusion for ice is ~3×10^5 J kg^{-1}; e.g., Nielsen, 1937; Cuffey and Paterson, 2010). But, making steam requires an order of magnitude more energy (~2.8×10^6 J kg^{-1}). Thus steam production requires significant rapid cooling of lava. It also assumes that meltwater produced by melting of ice remains at the point of contact long enough for energy from lava cooling to convert the water to steam. In general, flow of water in snowpack based on Darcy's Law gives typical values for downward water velocities of 0.5–5 × 10^{-5} m s^{-1} (DeWalle and Rango, 2008) assuming a constant porosity; this is of the same order of magnitude as the rates of melting by heat conduction (e.g., Wilson

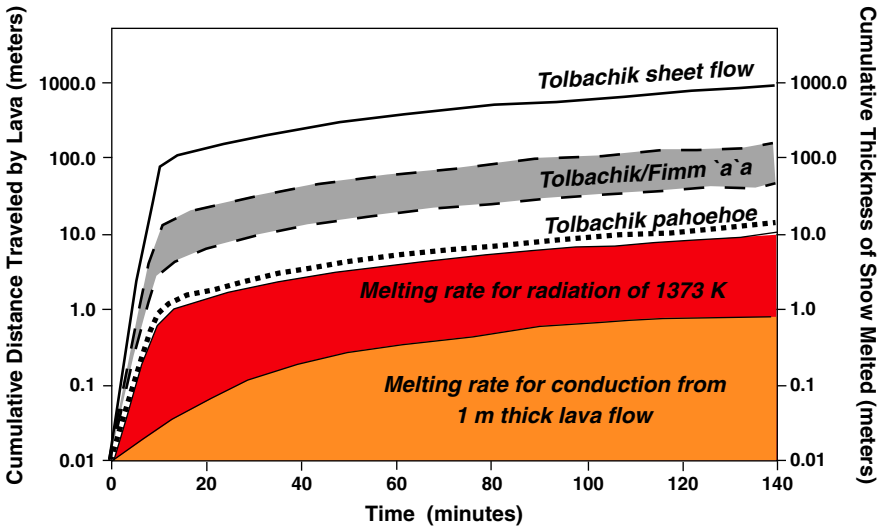

Fig. 8. Time versus distance for typical lava advance rates observed at Tolbachik and at 2010 Fimmvorduháls, Iceland (left Y-axis) compared with rates of snow melting predicted for radiant and conductive heat transfer (right Y-axis). Rate for sheet flow is shown by the uppermost, solid line, range of rates for `a`a lava by shading and bounding dashed lines, and rate for pahoehoe by the dotted line.

and Head, 2007; Fig. 8), which is consistent with the observation of limited steaming except for sub-snow lavas. Thus, unless the snow has a very low porosity, meltwater produced at the contact may be able to migrate away from the contact down into the snowpack essentially as fast as long-term (hours) heat transfer. We saw steam production at the front of advancing `a`a flows only when incandescent blocks fell directly onto the snow, where radiant heat transfer was fast enough to produce steam (e.g, Fig. 3D).

At Tolbachik the largest steam plumes formed where lava flows moved beneath the snow and then inflated. In those locations, melting was by radiation and conduction as lava came into direct contact with the snow, and, because the lavas were beneath snow, all the meltwater produced drained onto lava. Theoretically, one cubic meter of lava (density of ~2000 kg m^{-3} based on a lava density of ~2600 kg m^{-3} and an average vesicularity of 25%) could melt ~20 m^3 of snow with a density of ~450 kg m^{-3}, or convert 2.2 m^3 of snow into steam. This is consistent with the copious steam production seen where lava migrated beneath the snow.

4.3. What causes phreatic/phreatomagmatic explosions?

Previously explosive lava–ice/snow interactions have been documented at Klyuchevskoy volcano and at Mount Etna where lava flows on steep slopes collapsed and mixed with snow and ice (Belousov et al., 2011). We witnessed phreatic/phreatomagmatic explosions during April 2013 at Tolbachik (Fig. 9). The explosions occurred in the medial/distal part of the Tolud lava field, on a relatively broad area of flat terrain where slow `a`a flows advanced across relatively thick (>3 m) snow. A snow pit at this location had water-saturated snow at a depth of 1.6 m, and we encountered transient meltwater pockets in the snow (Fig. 7I). The event began with loud hissing as steam was released from fractures in the lava, and produced a steam/ash plume ~300 m high (Fig. 9A). Lapilli- and ash-sized fragments were ejected and were found in the snow adjacent to the lava flow edge. A simple model is the following (Fig. 9B). (1) Slow `a`a lava flows across an area of low gradient melting underlying snow. (2) Because of the low gradient meltwater collects at the bottom of the snowpack. (3) Inflation thickens the `a`a flow. (4) The thickening mass of lava eventually exceeds the strength of the water-saturated snow and the lava collapses into the slush. The resulting direct contact between lava and water produces steam that fractures the overlying lava and ejects lapilli and ash.

4.4. Is lava–snowpack interaction likely to make a recognizable record?

Few direct observations have verified that lava–ice/snow contact produces recognizable deposits. Edwards et al. (2012) suggested that records of those interactions were likely to be subtle. However, lava textures made during experiments do have distinctive morphologies (Edwards et al., 2013b). We recognized three unique features in sub-snow pahoehoe at Tolbachik (Fig. 10A). (1) Their upper surfaces have anomalously thick glassy rinds (up to 3 cm thick) with some hyaloclastite fragments. (2) Individual lava lobes have distinctly bulbous shapes. (3) Compound lava flows comprise dozens of small lobes that collectively have anomalously high profiles. The combination of all three makes a recognizable deposit that has a high preservation potential. While these distinctive morphologies have not been reported in the small body of literature on lava–snow interactions, the bulbous shapes are very similar to those produced during large-scale lava–snow/ice experiments (Edwards et al., 2013b).

At a broader scale, the combination of supra-snowpack `a`a lava and sub-/intra-snowpack pahoehoe lava makes a complex within-lava-field stratigraphy, especially in medial and distal areas (Fig. 10B). For example, after January 2013 the local snow had 3–4 layers of tephra. As later supra-snow `a`a lavas melted through the snow over a period of days, the relative stratigraphic position of the tephra (older) and the `a`a flow (younger) was preserved. However, sub-snow emplacement of later pahoehoe flows created an inverted stratigraphy; as the lavas melted up through the snow, older tephra melted out of the snowpack on top of the younger lava. Minor hyaloclastite created at the lava–snow interface by chilling also mixed in with the older tephra as snow melted. Thus an adjacent `a`a lava, even though it was older, might mistakenly be identified as having been emplaced after the pahoehoe flow, which was younger, based on the relative positions of the tephra (below the `a`a lava but on top of the pahoehoe lava). As the initial tephra was compositionally distinct from later lava (Volynets et al., 2013, 2015), the stratigraphic inversion (older tephra on younger lava) could confuse interpretations of initial lava compositions and magma dynamics. Because the sequence of lava emplacement was observed at Tolbachik, these relationships are easily distinguished. But at the older lava fields with incomplete exposure or preservation, such relationships would be less easily sorted.

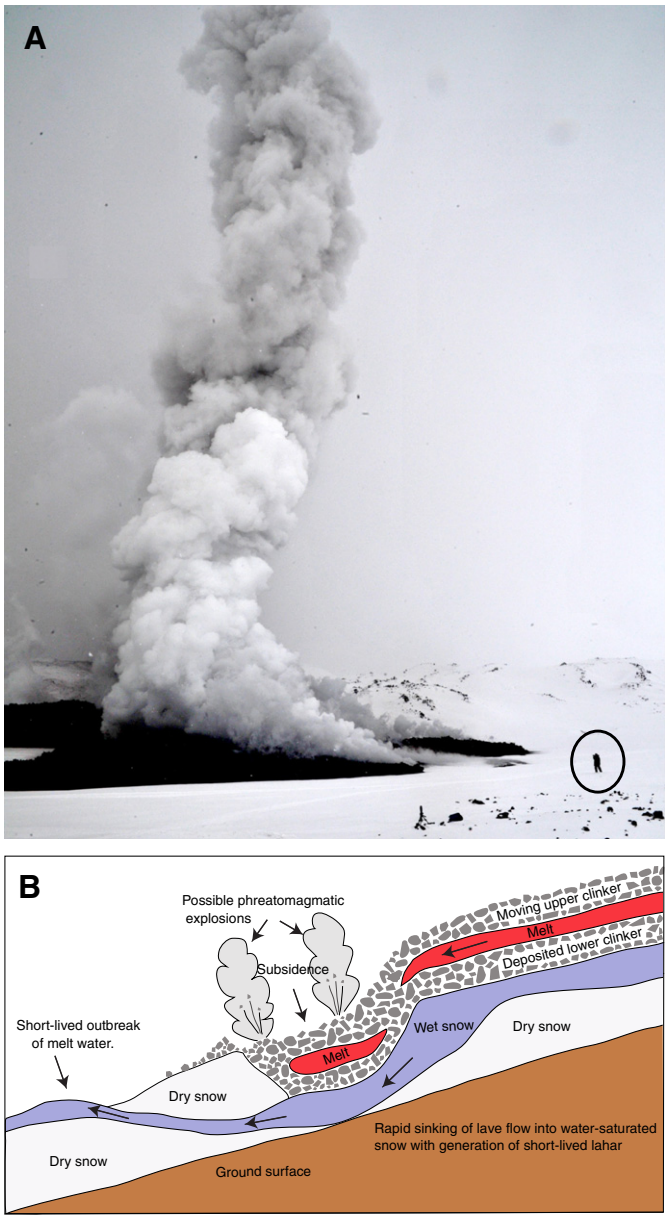

Fig. 9. Explosive interaction between `a`a flow and snowpack. A. Steam and ash plume produced by small explosion as `a`a lava flow collapsed into water-saturated snow. Person for scale. B. Schematic diagram showing an interpretation of the process responsible for the explosion.

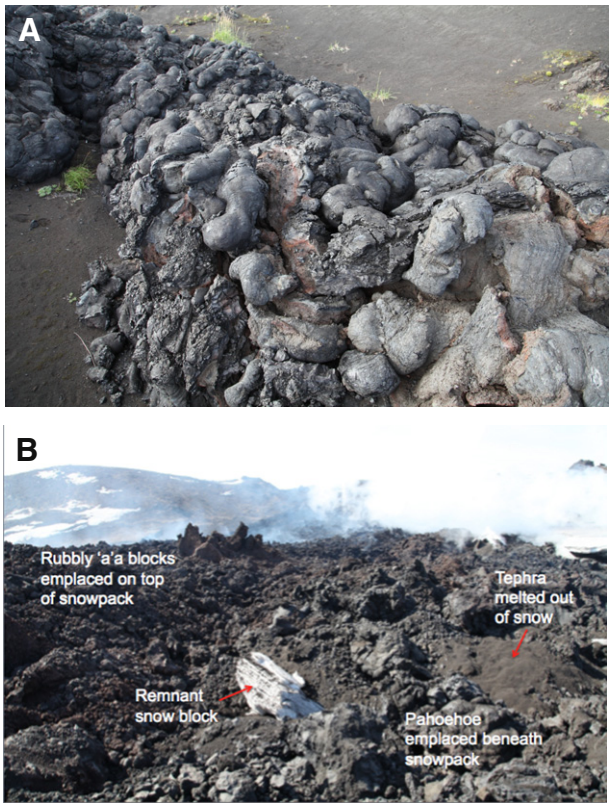

Fig. 10. Field images of unique deposits formed from lava–snowpack interactions. A. Bulbous lava morphologies in pahoehoe flows emplaced beneath snow. B. Inverted volcanic stratigraphy with younger pahoehoe lava covered by older tephra melted out of snow.

5. Conclusions

The 2012–13 Tolbachik fissure eruption provided excellent opportunities for close observation of lava–snow interactions. All three major lava morphologies (`a`a, sheet, pahoehoe) made direct contact with snow, although the products of interactions varied from nothing to distinct lava morphologies to phreatic/phreatomagmatic explosions. Measured lava velocities and thermal modeling are consistent with observations that lavas can migrate easily over snow, even upslope. Only slow lava emplacement, dominated by inflation, allows lavas to move through/beneath snow. We observed physical (compression and folding, extension and uplift) and thermal (local meltwater and steam production) snow responses to interactions with lava, including steaming where meltwater drained directly onto lava surfaces, and phreatic/phreatomagmatic explosions where gradients allowed meltwater to collect beneath thickening lavas. Whereas most of the effusive deposits preserve little direct evidence for snow presence, the sub-snow lavas have distinct morphologies that should be recognizable at other volcanoes. If so, we will be able to better evaluate possible seasonal effects on eruptions and document climate-controlled changes in snowlines at snow-clad volcanoes.

Acknowledgments

Funding for this research is from the National Science Foundation (NSF-RAPID 0910712 to BRE), the National Geographic Committee for Research (9152-12 to BRE), and the Institute of Volcanology and Seismology, Petropavlovsk, Russia. We thank Y. Demyanchuk, S. Chirkov, Y. Bukatov and S. Mikaelov for their assistance in the field, and A. Bichenko, Y. Demianchuk, P. Izbekov, A. Sokorenko and D. Savelyev for sharing their field observations. An encouraging review by J. W. Head and an exhaustive review by R. Waitt helped us to shorten and clarify the manuscript significantly.

References

Allen, C.C., 1979. Volcano–ice interactions on Mars. J. Geophys. Res. 84, B14. http://dx.doi.org/10.1029/JB084iB14p08048.
Belousov, A., Behncke, B., Belousova, M., 2011. Generation of pyroclastic flows by explosive interaction of lava flows with ice/water-saturated substrate. J. Volcanol. Geotherm. Res. 202, 60–72.
Belousov, A., Belousova, M., Edwards, B.R., Volynets, A., Melnikov, D., 2015. Overview of the precursors and dynamics of the 2012–13 basaltic fissure eruption of Tolbachik volcano, Kamchatka, Russia. J. Volcanol. Geotherm. Res. 307, 22–37.
Cousins, C.R., Crawford, I.A., Carrivick, J.L., Gunn, M., Harris, J., Kee, T.P., Karlsson, M., Carmody, L., Cockell, C., Herschy, B., Joy, K.H., 2013. Glaciovolcanic hydrothermal environments in Iceland and implications for their detection on Mars. J. Volcanol. Geotherm. Res. 256, 61–77.
Cuffey, K.M., Paterson, W.S.B., 2010. Physics of Glaciers. Elsevier, Burlington MA (693 pp.).
DeWalle, D.R., Rango, A., 2008. Principles of Snow Hydrology. Cambridge Univ Press, Cambridge (410 pp.).
Edwards, B.R., Tuffen, H., Skilling, I., Wilson, L., 2009. Introduction to special issue on volcano–ice interactions on Earth and Mars: the state of the science. J. Volcanol. Geotherm. Res. 185, 247–250.
Edwards, B.R., Russell, J.K., Simpson, K., 2011. Volcanology and petrology of Mathews Tuya, northern British Columbia, Canada: glaciovolcanic constraints on interpretations of the 0.730 Ma Cordilleran paleoclimate. Bull. Volcanol. http://dx.doi.org/10.1007/s00445-010-0418-z.
Edwards, B.R., Magnússon, E., Thordarson, T., Gudmundsson, M.T., Höskuldsson, A., Oddsson, B., Haklar, J., 2012. Interactions between lava and snow/ice during the 2010 Fimmvörðuhals eruption, south-central Iceland. J. Geophys. Res. 117, B04302.
Edwards, B.R., Belousov, A., Belousova, M., Volynets, A., Melnikov, D., Chirkov, S., Senyukov, S., Gordeev, E., Muraviev, Y., Izbakov, I., 2013a. Another 'Great Tolbachik' eruption? EOS Trans. Am. Geophys. Union 94, 189–191. http://dx.doi.org/10.1002/2013EO210002 (21 May 2013).
Edwards, B.R., Karson, J., Wysocki, R., Lev, E., Bindeman, I., Kueppers, U., 2013b. Constraints on lava–ice interactions from large scale experiments. Geology 41, 851–854.
Edwards, B.R., Belousov, A., Belousova, M., 2014. Propogation style controls lava–snow interactions. Nat. Commun. 5, 5666. http://dx.doi.org/10.1038/natcomms6666.
Edwards, B.R., Russell, J.K., Gudmundsson, M.T., 2015. Chapter 20. Glaciovolcanism. In: Sigurdsson, et al. (Eds.), Encyclopedia of Volcanoes, 2nd edition.
Einarsson, T., 1949. The flowing lava: studies of its main physical and chemical characteristics. Societas Scientiarum Islandica. Visindafdag Islendiga, Reykjavik, pp. 1–70.
Gronvold, K., Larsen, G., Einarsson, P., Thorarinsson, S., Saemundsson, K., 1983. The 1980–81 Hekla eruption. Bull. Volc. 46, 349–363.
Gualda, G.A.R., Ghiorso, M.S., Lemons, R.V., Carley, T.L., 2012. Rhyolite-MELTS: a modified calibration of MELTS optimized for silica-rich, fluid-bearing magmatic systems. J. Petrol. 53, 875–890.
Gudmundsson, M.T., Sigmundsson, F., Björnsson, H., 1997. Ice–volcano interaction of the 1996 Gjálp subglacial eruption, Vatnajökull, Iceland. Nature 389, 954–957.
Gudmundsson, M.T., Sigmundsson, F., Björnsson, H., Högnadóttir, D., 2004. The 1996 eruption at Gjálp, Vatnajökull ice cap, Iceland—efficiency of heat transfer, ice deformation and subglacial water pressure. Bull. Volcanol. 66, 46–65.
Gudmundsson, M.T., Larsen, G., Hoskuldsson, A., Gylfason, A.G., 2008. Volcanic hazards in Iceland. Jökull 58, 251–268.
Gudmundsson, M.T., Thordarson, T., Hoskuldsson, A., Larsen, G., Bjornsson, H., Prata, F.J., Oddsson, B., Magnusson, E., Hognadottir, T., Petersen, G.N., Hayword, C.L., Stevenson, J.A., Jonsdottir, I., 2012. Ash generation and distribution from the April–May 2010 eruption of Eyjafjallajokull, Iceland. Nat. Sci. Rep. http://dx.doi.org/10.1038/srep00572.
Head, J.W., Wilson, L., 2007. Heat transfer in volcano–ice interactions on Earth: synthesis of environments and implications for processes and landforms. Ann. Glaciol. 45, 1–13.
Höskuldsson, A., Sparks, R.S.J., 1997. Thermodynamics and fluid dynamics of effusive subglacial eruptions. Bulletin of Volcanology 59, 219–230.
Hungerford, J.D.G., Edwards, B.R., Skilling, I.P., Cameron, B., 2014. Evolution of a Subglacial Basaltic Lava Flow Field: Tennena Cone volcanic center, Mount Edziza Volcanic Complex, British Columbia, Canada. J. Volc. Geotherm. Res. 272, 39–58. http://dx.doi.org/10.1016/j.jvolgeores.2013.09.012.
Jude-Eton, T.C., Thordarson, T., Gudmundsson, M.T., Oddsson, B., 2012. Dynamics, stratigraphy and proximal dispersal of supraglacial tephra during the ice-confined 2004 eruption at Grímsvötn Volcano, Iceland. Bull. Volcanol. 74, 1057–1082.
Kjartansson, G., 1951. Water flood and mudflows. In: Einarsson, T., Kjartansson, G., Thorarinsson, S. (Eds.), The eruption of Hekla 1947–1948. Visindafélag Islendinga (Societas Scientiarum Islandica), Reykjavík ((II, 4), 51 p. and 8 plates).
Magnusson, E., Guðmundsson, M.T., Roberts, M.T., Sigurdsson, G., Hoskuldsson, F., Oddsson, B., 2012. Ice–volcano interactions during the 2010 Eyjafjallajokull eruption, as revealed by airborne imaging radar. J. Geophys. Res. http://dx.doi.org/10.1029/2012JB009250.
Major, J.J., Newhall, C.G., 1989. Snow and ice perturbation during historical volcanic eruptions and the formation of lahars and floods. Bull. Volcanol. 52, 1–27.
McGarvie, D.W., Burgess, R., Tindle, A.J., Tuffen, H., Stevenson, J.A., 2006. Pleistocene rhyolitic volcanism at the Torfajökull central volcano, Iceland: eruption ages, glaciovolcanism, and geochemical evolution. Jökull 56, 57–75.

Moreno, H.R., Fuentealba, G.C., 1994. The May 17–19 1994 Llaima volcano. Revista geologica de Chile 21, 167–171.
Naranjo, J.A., Moreno, H., 2004. Laharic debris-flows from Villarrica Volcano. Boletín Servicio Nacional de Geología y Minería 61, 28–38.
Naranjo, J.A., Moreno, H., Banks, N.G., 1993. La erupción del volcán Hudson en l991 (467S). Región XI, Aisén, Chile. Serv Nac Geol Minería Boletin 44, 1–50.
Nielsen, N., 1937. A volcano under an ice-cap, Vatnajokull, Iceland, 1934–36. Geogr. J. 90, 6–23.
Oddsson, B., Gudmundsson, M.T., Hognadottir, T., Magnusson, E., Hoskuldsson, F., 2012. Lava-ice interaction during the advance of a trachyandesitic lava flow down the Gígjökull outlet glacier in the April-May 2010 Eyjafjallajökull eruption. Iceland, EOS-Abstracts with Programs, NH11B-1131 2010.
Roberts, M.J., 2005. Jökulhlaups: a reassessment of floodwater flow through glaciers. Rev. Geophys. 43, 147–168.
Rowland, S.K., Walker, G.P.L., 1987. Toothpaste lava: characteristics and origin of a lava structural type transitional between pahoehoe and aa. Bull. Volc. 49, 631–641.
Scanlon, K.E., Head III, J.W., Wilson, L., Marchant, D.R., 2014. Volcano–ice interactions in the Arsia Mons tropical mountain glacier deposits. Icarus 237, 315–339. http://dx.doi.org/10.1016/j.icarus.2014.04.024.
Scanlon, K.E., Head III, J.W., Marchant, D.R., 2015. Volcanism-induced, local wet-based glacial conditions recorded in the Late Amazonian Arsia Mons tropical glacier deposits. Icarus 250, 18–31. http://dx.doi.org/10.1016/j.icarus.2014.11.016.
Schmid, A., Sonder, I., Seegelken, R., Zimanowski, B., Büttner, R., Gudmundsson, M.T., Oddsson, B., 2010. Experiments on the heat discharge at the dynamic magma–water-interface. Geophys. Res. Lett. 37, L20311. http://dx.doi.org/10.1029/2010GL044963.
Smellie, J.L., Johnson, J.S., McIntosh, W.C., 2008. Six million years of glacial history recorded in volcanic lithofacies of the James Ross Island Volcanic Group, Antarctic Peninsula. Palaeogeogr. Palaeoclimatol. Palaeoecol. 260, 122–148.
Spera, F., 2000. Physical properties of magma. In: Sigurdsson, H. (Ed.)Encyclopedia of Volcanoes. Academic Press, San Diego, pp. 171–190.
Tuffen, H., Betts, R., 2010. Volcanism and climate: chicken and egg (or vice versa)? Philos. Trans. R. Soc. Lond. A 368, 2585–2588.
Volynets, A., Melnikov, D., Yakushev, A., 2013. First data on composition of the volcanic rocks of the IVS 50th anniversary Fissure Tolbachik Eruption. Dokl. Earth Sci. 452, 953–957.
Volynets, A., Edwards, B., Melnikov, B., Yakushev, A., Griboedova, I., 2015. Monitoring of the volcanic rock compositions during the 2012–2013 fissure eruption at Tolbachik volcano, Kamchatka. J. Volcanol. Geotherm. Res. 307, 120–132.
Waythomas, C.F., Pierson, T.C., Major, J.J., Scott, W.E., 2013. Voluminous ice-rich and water-rich lahars generated during the 2009 eruption of Redoubt Volcano, Alaska. J. Volcanol. Geotherm. Res. 239, 389–413.
Wilson, L., Head, J.W., 2007. Heat transfer in volcano–ice interactions on Earth. Ann. Glaciol. 45, 83–86.
Wilson, L., Smellie, J.L., Head, J.W., 2014. Chapter 13. Volcano–ice interactions. In: Fagent, S.A., Gregg, T.K.P., Lopes, R.M.C. (Eds.), Modeling Volcanic Processes. Cambridge Univ. Press, pp. 275–299.